Readout of a single electron spin in a double quantum dot using a quantum point contact

2008 J. Phys.: Condens. Matter 20 395206

(http://iopscience.iop.org/0953-8984/20/39/395206)

J. Phys.: Condens. Matter **20** (2008) 395206 (11pp) doi:10.1088/0953-8984/20/39/395206

Readout of a single electron spin in a double quantum dot using a quantum point contact

Jian-Ping Zhang[1], **Shi-Hua Ouyang**[1,2], **Chi-Hang Lam**[2] **and J Q You**[1]

[1] Department of Physics and Surface Physics Laboratory (National Key Laboratory), Fudan University, Shanghai 200433, People's Republic of China
[2] Department of Applied Physics, Hong Kong Polytechnic University, Hung Hom, Hong Kong, People's Republic of China

Received 15 March 2008, in final form 6 August 2008
Published 1 September 2008
Online at stacks.iop.org/JPhysCM/20/395206

Abstract

We study the dynamics of a single electron spin in a double quantum dot (DQD) and its readout via a quantum point contact (QPC). We model the system microscopically and derive rate equations for the reduced electron density matrix of the DQD. Two cases with one and two electrons in the DQD are studied. In the one-electron case, with different Zeeman splittings in the two dots, the electron spin states are distinctly characterized by a constant and an oscillatory current through the QPC. In the two-electron case, the readout of the spin state of the electron in one of the dots called the qubit dot is essentially similar after considering hyperfine interactions between the electrons and the nuclear spins of the host materials and a uniform magnetic field applied to the DQD. Moreover, to ensure that an electron is properly injected into the qubit dot, we propose to determine the success of the electron injection from the variations of the QPC current after applying an oscillating magnetic field to the qubit dot.

(Some figures in this article are in colour only in the electronic version)

1. Introduction

A single or a small number of electron spins confined in a semiconductor quantum dot (QD) has become a subject of considerable interest, partly motivated by potential applications in quantum information processing. Because a electron spin in a QD can have a relatively long decoherence time, it is a promising candidate for realizing a qubit [1, 2], the basic unit of a quantum computer. For a single electron spin, the dephasing time is found in theory to be microseconds in both GaAs [3, 4] and InAs dots [5]. Experimental results show that the ensemble dephasing time of an electron spin has the order of nanoseconds [6, 7]. Moreover, the spin relaxation time in a large GaAs dot is found to be about 1–10 μs at a moderately low temperature of 10 K [8]. Indeed, recent experiments have demonstrated that spins in QDs can be used to carry quantum information [9–11]. For both applications in quantum computing and fundamental research, the readout of qubit states based on electron spin is a centrally important issue [12]. However, due to the weak magnetic moment associated with the electron spin, it is difficult to directly measure the electron spin states. A possible solution is to correlate the spin states to charge states, and the measurement of the charge on the dot will provide information about the original spin states [2]. This can be implemented using a quantum point contact (QPC), which is a charge detector and can be used to determine the number variation of the electrons confined in the QD.

Recently, the readout of electron spin states in a QD has been realized using such a spin–charge conversion [10, 13]. For the experiment in [10], a QD is connected to an electron reservoir. Applying an external magnetic field, gate voltages are applied so that the electron confined in the dot can tunnel to the reservoir if its spin is down. (A spin-up electron cannot tunnel in this case.) A nearby QPC is used to detect the electron number variation in this QD and can determine the electron spin state in the QD. Also, Engel *et al* [14] proposed various implementations of the readout process based on a double quantum dot (DQD). Barrett and Stace [15] proposed

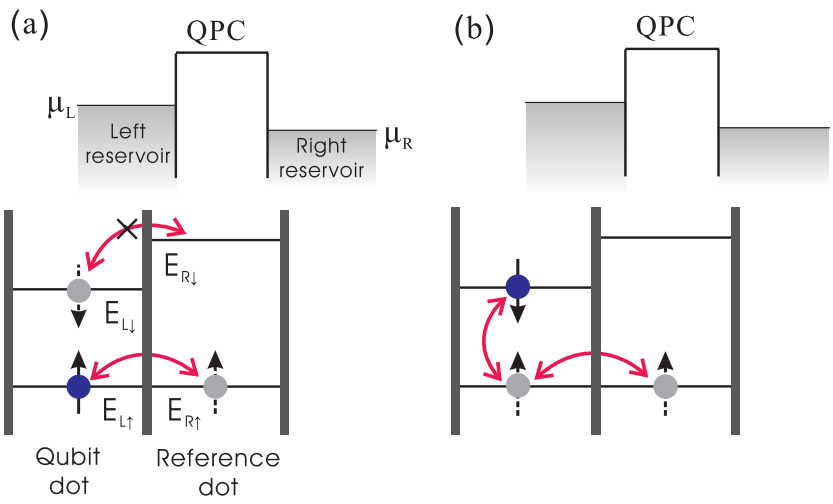

Figure 1. Schematic diagram of a double quantum dot (DQD) and a quantum point contact (QPC) with only one electron in the DQD. The left (qubit) dot of the DQD is coupled to a right (reference) dot via hopping. The nearby QPC is used as a detector measuring the number variation of electrons in the reference dot. An energy-level detuning of the electron spin states is generated using two external magnetic fields in the two dots. (a) Gate voltages are adjusted to keep $E_{L\uparrow} = E_{R\uparrow}$, so that the hopping of the spin-up electron between the left and right dot is allowed. Moreover, the energy-level detuning for the spin-down electron is much larger than the hopping strength, i.e., $E_{R\downarrow} - E_{L\downarrow} \gg \Omega_0$, and hence the hopping of the spin-down electron between the two dots is forbidden. (b) The hopping blockade for the spin-down electron is lifted by applying a transverse magnetic field $B(t) = B_L^x \cos(\omega_c t)$ to the left dot, which flips the electron spin.

a electron spin readout approach using a microwave field and an inhomogeneous Zeeman splitting across the DQD.

In the present paper, we study two implementations for reading-out electron spin states based on a DQD coupled to a QPC. Also, we explain the effects of static and oscillating magnetic fields on the electron spin states. The first implementation involves a single electron in the DQD. The readout of the spin states is based on the different Zeeman splittings in the two QDs. In the second implementation, two electrons are allowed in the DQD. The Pauli exclusion principle and hyperfine interactions between the electrons in the DQD and the nuclear spins in the host materials enable the readout of the electron spin states. These are interesting examples for implementing readout of the electron spin states. A potential advantage of our proposal is that the readout manipulation can easily be switched on (off) by decreasing (increasing) the tunneling barrier between the two dots through varying the gate voltages. Thus, the readout process can be implemented only when needed. This is important in quantum information processing. To understand the underlying physics from a microscopic point of view, we derive a set of rate equations describing the electron dynamics of the DQD system. Based on these rate equations, we calculate the QPC current and illustrate that the QPC current behaves differently for different spin states.

The paper is organized as follows. In section 2, we model the system when only one electron is confined in the DQD. A set of Bloch-type rate equations are derived to describe the detailed measurement processes for the electron spin states in the qubit dot. In section 3, we study the measurement of the electron spin states in the qubit dot when two electrons are confined in the DQD. Section 4 is the conclusion.

2. Readout of single electron spin: one electron in DQD

2.1. Theoretical model

We first discuss a scheme to detect the electron spin states in the case with only one electron confined in the DQD. As schematically shown in figure 1, the whole system consists of a DQD and a QPC. The left dot is used as a qubit dot, in which the electron spin is expected to be read out. The right dot is used as a reference dot. The QPC is capacitively coupled to the right dot and serves as a readout device. The electron number variation in the right dot induces a change in the barrier in the QPC. This leads to a variation of the current through the QPC, which can be used to indicate the occupation of the right dot [16].

The Hamiltonian of the whole system is given by

$$H = H_{\rm DQD} + H_{\rm QPC} + H_{\rm int} + H_{\rm rf}, \tag{1}$$

with

$$H_{\rm DQD} = \sum_{i\sigma} E_{i\sigma} c_{i\sigma}^{\dagger} c_{i\sigma} + \sum_{\sigma} \Omega_0 (c_{{\rm L}\sigma}^{\dagger} c_{{\rm R}\sigma} + c_{{\rm R}\sigma}^{\dagger} c_{{\rm L}\sigma}), \tag{2}$$

where $i = {\rm L}, {\rm R}$ denote the left and right dots, and $c_{i\sigma}^{\dagger}$ ($c_{i\sigma}$) is the creation (annihilation) operator of electron with spin σ in the ith QD. Ω_0 denotes the hopping amplitude between the two dots and here it is assumed to be spin-independent. We have denoted the energy levels in the ith dot by $E_{i\uparrow(\downarrow)} = E_i \mp \frac{1}{2}\Delta_i^z$, with $\Delta_i^z = g\mu_{\rm B} B_i^z$, where E_i is the orbital energy level of the QD and B_i^z is an externally applied magnetic field in the ith dot along the z direction. Here, g is the effective gyromagnetic factor and $\mu_{\rm B}$ is the Bohr magneton. We have chosen the unit

$\hbar = 1$. The Hamiltonian of the QPC reads

$$H_{\rm QPC} = \sum_{\alpha k} E_{\alpha k} a^\dagger_{\alpha k} a_{\alpha k} + \sum_{lrk} \Omega_{lr} \left(a^\dagger_{lk} a_{rk} + a^\dagger_{rk} a_{lk} \right), \quad (3)$$

where $a^\dagger_{\alpha k}$ ($a_{\alpha k}$) is the creation (annihilation) operator of an electron with momentum k in reservoir α ($\alpha = l, r$). $H_{\rm int}$ gives the electrostatic interaction between the DQD and the QPC:

$$H_{\rm int} = \sum_{lrk\sigma} \delta\Omega_{lr} c^\dagger_{{\rm R}\sigma} c_{{\rm R}\sigma} (a^\dagger_{lk} a_{rk} + a^\dagger_{rk} a_{lk}). \quad (4)$$

An electron spin resonance (ESR) magnetic field is applied in the x direction at the left dot, leading to a term

$$H_{\rm rf} = \Delta_x(t)(c^+_{{\rm L}\uparrow} c_{{\rm L}\downarrow} + {\rm H.c.}) \quad (5)$$

with $\Delta_x(t) = \frac{1}{2} g \mu_{\rm B} B^x_{\rm L} \cos(\omega_{\rm c} t)$. This ESR magnetic field generates spin flipping when it is resonant with the Zeeman splitting on the left dot, i.e., $\omega_{\rm c} = g\mu_{\rm B} B^z_{\rm L}$.

The spin-up and spin-down states $|\uparrow_{\rm L}\rangle$ and $|\downarrow_{\rm L}\rangle$ in the left dot constitute the basis states of a qubit. The right dot works as a reference dot, the electron occupation of which is measured by the nearby QPC. Energy detuning for the spin-up (-down) electron is $\varepsilon_{\uparrow(\downarrow)} = E_{{\rm R}\uparrow(\downarrow)} - E_{{\rm L}\uparrow(\downarrow)}$. We assume that the Zeeman splittings Δ^z_i are different in the two dots. This can be realized, e.g., by applying a micro-size permanent magnet near one dot of the DQD [17]. This leads to a difference $\varepsilon_\uparrow - \varepsilon_\downarrow = \Delta^z_{\rm R} - \Delta^z_{\rm L}$ in the energy-level splittings for the spin-up and spin-down electrons. In our consideration, gate voltages are adjusted to keep $\varepsilon_\uparrow \approx 0$, so that a spin-up electron can hop back and forth between the two dots. Furthermore, we also assume $\varepsilon_\downarrow \gg \varepsilon_\uparrow, \Omega_0$, so that hopping is forbidden for spin-down electrons. However, this spin blockade can be lifted by an ESR magnetic field. Here, in the one-electron case, the effects of the nuclear magnetic fields in the two dots are neglected. This is because the Zeeman splitting in each dot is much larger than the nuclear field in the x and y directions. Moreover, the z component of the nuclear field only shifts the energy level and can be included in the Zeeman splitting.

The physical picture of the electron spin readout is as follows. We first inject an electron with either up or down spin into the qubit (left) dot. An initially spin-up electron in the qubit dot can hop into the reference dot. This will lead to a variation of the current through the QPC. In contrast, for an initially spin-down electron in the qubit dot, it will remain stationary because $\varepsilon_\downarrow \gg \Omega_0$. As a result, no variation in the QPC current occurs. Therefore, one can determine the initial electron spin state based on the variation of the current through the QPC. However, in practical experiments, the injection of electrons into the DQD may not be always successful. Without any electron in the DQD, there is also no variation in the QPC current. Thus, this simple implementation cannot distinguish between the cases with zero or one spin-down electron. To solve this problem, as will be shown below, one can apply an ESR magnetic field in the qubit dot. The ESR magnetic field induces spin flipping in the left dot. If there is a spin-down electron, it can be converted to the spin-up state by the ESR field and then hop onto the right dot. Therefore, a current variation will be observed in the QPC. In contrast, the QPC current will remain unchanged in the zero-electron case even in the presence of the ESR field.

2.2. Bloch-type rate equation

To describe the physical processes quantitatively, we derive a set of Bloch-type rate equations for the reduced density matrix $\sigma(t)$ of the DQD system. Following Gurvitz *et al* [18, 19], we write the wavefunction of the whole system in the occupation representation as

$$\begin{aligned} |\Psi(t)\rangle = \sum_\sigma \Big[& b_{{\rm L}\sigma}(t) c^\dagger_{{\rm L}\sigma} + b_{{\rm R}\sigma}(t) c^\dagger_{{\rm R}\sigma} \\ & + \sum_{lr} b_{{\rm L}\sigma lr}(t) c^\dagger_{{\rm L}\sigma} a^\dagger_r a_l + \sum_{lr} b_{{\rm R}\sigma lr}(t) c^\dagger_{{\rm R}\sigma} a^\dagger_r a_l \\ & + \sum_{l<l', r<r'} b_{{\rm L}\sigma ll'rr'}(t) c^\dagger_{{\rm L}\sigma} a^\dagger_r a^\dagger_{r'} a_l a_{l'} \\ & + \sum_{l<l', r<r'} b_{{\rm R}\sigma ll'rr'}(t) c^\dagger_{{\rm R}\sigma} a^\dagger_r a^\dagger_{r'} a_l a_{l'} + \cdots \Big] |0\rangle, \end{aligned} \quad (6)$$

where $b_j(t)$, $j = {\rm L}\sigma, {\rm R}\sigma, {\rm L}\sigma lr, {\rm R}\sigma lr, \ldots$. are the time-dependent probability amplitudes to find the system in the corresponding states. For example, $b_{{\rm L}\sigma lr}(t)$ denotes the probability amplitude for the state with an electron having tunneled through the QPC barrier (from the left reservoir to the right one) at time t, and an extra electron with spin σ staying in the left dot. The vacuum state $|0\rangle$ corresponds to the state where there is no extra electron in the DQD and all the energy levels up to the Fermi energies $\mu_{\rm L}$ and $\mu_{\rm R}$ of the two reservoirs of the QPC are occupied by electrons.

The relevant electron states of the DQD span a four-dimensional Hilbert space. We adopt the notations $|1\rangle \equiv |\uparrow_{\rm L}\rangle$ and $|2\rangle \equiv |\downarrow_{\rm L}\rangle$ for the left-dot states, as well as $|3\rangle \equiv |\uparrow_{\rm R}\rangle$ and $|4\rangle \equiv |\downarrow_{\rm R}\rangle$ for the right-dot states. A diagonal element $\sigma_{ii}(t)$ ($i = 1, 2, 3, 4$) of the reduced matrix represents the occupation probability of the state $|i\rangle$, while an off-diagonal element $\sigma_{ij}(t)$ characterizes the quantum coherence. Each σ_{ii} is further given by

$$\sigma_{ii}(t) = \sigma^{(0)}_{ii} + \sigma^{(1)}_{ii} + \sigma^{(2)}_{ii} + \cdots, \quad (7)$$

where $\sigma^{(n)}_{ii}$ is the probability that the DQD is at state $|i\rangle$ after n electrons have tunneled from the left reservoir of the QPC to the right one. In this notation, we have, for example

$$\begin{aligned} \sigma^{(0)}_{11} &= |b_{{\rm L}\uparrow}(t)|^2, \\ \sigma^{(1)}_{11} &= \sum_{lr} |b_{{\rm L}\uparrow lr}(t)|^2, \\ \sigma^{(2)}_{11} &= \sum_{l<l', r<r'} |b_{{\rm L}\uparrow ll'rr'}|^2, \ldots. \end{aligned} \quad (8)$$

The current flowing through the QPC is

$$I_{\rm QPC}(t) = e \frac{{\rm d}N(t)}{{\rm d}t}, \quad (9)$$

where $N(t)$ is the number of electrons transported to the right reservoir of the QPC at time t. Accordingly, we have

$$I_{\rm QPC}(t) = \sum_{n,i} n \dot{\sigma}^{(n)}_{ii}(t). \quad (10)$$

Substituting the many-body wavefunction of the whole system into the Schrödinger equation ${\rm i}|\dot{\psi}(t)\rangle = H|\psi(t)\rangle$, one gets a set of differential equations for the probability

amplitudes $b_j(t)$. In the nonequilibrium transport in the QPC with a large voltage bias, following [19] and [20], the Bloch-type rate equations for the reduced density matrix $\sigma(t)$ of the DQD are derived by integrating the degrees of freedom of the QPC reservoirs. By summing $\dot{\sigma}^{(n)}(t)$ over n, the rate equations for the diagonal elements are given by

$$\begin{aligned}
\dot{\sigma}_{11}(t) &= \mathrm{i}\Omega_0(\sigma_{13}-\sigma_{31}) + \mathrm{i}\Delta_x(t)(\sigma_{12}-\sigma_{21}),\\
\dot{\sigma}_{22}(t) &= \mathrm{i}\Omega_0(\sigma_{24}-\sigma_{42}) + \mathrm{i}\Delta_x(t)(\sigma_{21}-\sigma_{12}),\\
\dot{\sigma}_{33}(t) &= \mathrm{i}\Omega_0(\sigma_{31}-\sigma_{13}),\\
\dot{\sigma}_{44}(t) &= \mathrm{i}\Omega_0(\sigma_{42}-\sigma_{24}).
\end{aligned} \tag{11}$$

The rate equations for the off-diagonal elements are

$$\begin{aligned}
\dot{\sigma}_{12}(t) &= \mathrm{i}(E_{\mathrm{L}\downarrow}-E_{\mathrm{L}\uparrow})\sigma_{12} - \mathrm{i}\Omega_0\sigma_{32} + \mathrm{i}\Omega_0\sigma_{14}\\
&\quad + \mathrm{i}\Delta_x(t)(\sigma_{11}-\sigma_{22}),\\
\dot{\sigma}_{13}(t) &= \mathrm{i}(E_{\mathrm{R}\uparrow}-E_{\mathrm{L}\uparrow})\sigma_{13} + \mathrm{i}\Omega_0(\sigma_{11}-\sigma_{33}) - \mathrm{i}\Delta_x(t)\sigma_{23}\\
&\quad - \frac{\Gamma_\mathrm{d}}{2}\sigma_{13} - \frac{\chi}{2}\sigma_{11} - \frac{\chi}{2}\sigma_{33},\\
\dot{\sigma}_{14}(t) &= \mathrm{i}(E_{\mathrm{R}\downarrow}-E_{\mathrm{L}\uparrow})\sigma_{14} + \mathrm{i}\Omega_0\sigma_{12} - \mathrm{i}\Omega_0\sigma_{34} - \mathrm{i}\Delta_x(t)\sigma_{24}\\
&\quad - \frac{\Gamma_\mathrm{d}}{2}\sigma_{14} - \frac{\chi}{2}\sigma_{12} - \frac{\chi}{2}\sigma_{34},\\
\dot{\sigma}_{23}(t) &= \mathrm{i}(E_{\mathrm{R}\uparrow}-E_{\mathrm{L}\downarrow})\sigma_{23} + \mathrm{i}\Omega_0\sigma_{21} - \mathrm{i}\Omega_0\sigma_{43} - \mathrm{i}\Delta_x(t)\sigma_{13}\\
&\quad - \frac{\Gamma_\mathrm{d}}{2}\sigma_{23} - \frac{\chi}{2}\sigma_{21} - \frac{\chi}{2}\sigma_{43},\\
\dot{\sigma}_{24}(t) &= \mathrm{i}(E_{\mathrm{R}\downarrow}-E_{\mathrm{L}\downarrow})\sigma_{24} + \mathrm{i}\Omega_0(\sigma_{22}-\sigma_{44}) - \mathrm{i}\Delta_x(t)\sigma_{14}\\
&\quad - \frac{\Gamma_\mathrm{d}}{2}\sigma_{24} - \frac{\chi}{2}\sigma_{22} - \frac{\chi}{2}\sigma_{44},\\
\dot{\sigma}_{34}(t) &= \mathrm{i}(E_{\mathrm{R}\downarrow}-E_{\mathrm{R}\uparrow})\sigma_{34} + \mathrm{i}\Omega_0\sigma_{32} - \mathrm{i}\Omega_0\sigma_{14},
\end{aligned} \tag{12}$$

where $\Gamma_\mathrm{d} = (\sqrt{D'}-\sqrt{D})^2$ is the dephasing rate induced by the QPC detector [19]. Here we have defined

$$D = 2\pi\rho_\mathrm{L}\rho_\mathrm{R}\Omega^2 V_\mathrm{d}, \qquad D' = 2\pi\rho_\mathrm{L}\rho_\mathrm{R}\Omega'^2 V_\mathrm{d}, \tag{13}$$

and

$$\chi = \frac{\Lambda}{V_\mathrm{d}}\left(\frac{\Omega}{\Omega'} + \frac{\Omega'}{\Omega} - 2\right), \tag{14}$$

with $\Lambda = 2\pi\rho_\mathrm{L}\rho_\mathrm{R}\Omega'\Omega_0\Omega V_\mathrm{d}$. In equation (12), the terms proportional to χ are due to the inclusion of higher-order terms of $O(\Omega^2\Omega_0/V_\mathrm{d}^2)$ [20]. Also, we assume that the tunneling couplings depend weakly on the energy, so that $\Omega_{lr}(E_l, E_r) \equiv \Omega$, and $\Omega_{lr} + \delta\Omega_{lr} \equiv \Omega'$. $V_\mathrm{d} = \mu_\mathrm{L} - \mu_\mathrm{R}$ is the voltage bias applied on the QPC and $\rho_\mathrm{L}(\rho_\mathrm{R})$ is the density of states in the left (right) reservoir of the QPC. From equation (12), one can see that Γ_d characterizes the exponential damping of the off-diagonal density matrix elements. Now, the QPC current is given by

$$I_\mathrm{QPC}(t) = I_0[\sigma_{11}(t)+\sigma_{22}(t)] + I_1[\sigma_{33}(t)+\sigma_{44}(t)], \tag{15}$$

where $I_0 \equiv D$ is the current flowing through the QPC when the right dot of the DQD is empty, while $I_1 \equiv D'$ is the QPC current when the right dot is occupied by one electron. Since $I_0 \neq I_1$ in general, one can determine the electron occupation of the right dot from the variation of the QPC current.

We first consider the case without an ESR oscillating magnetic field, i.e., $\Delta_x(t) = 0$. Using equations (11) and (12), one can numerically calculate the occupation probabilities σ_{ii}, $i = 1$ to 4. A typical value for the hopping coupling between the two dots in experiments is $\Omega_0 = 0.25$ μeV [21]. We have taken parameters so that the initial current of the QPC is $I_0 = 1.5$ nA if the right dot is empty [10], while it equals $I_1 = 1$ nA if there is an electron in the right dot. First, consider the case that a spin-up electron is injected into the left dot. Figure 2(a) shows the calculated occupation probability of the electron in the right dot. The corresponding current flowing through the QPC is given in figure 2(c). It shows that the current I_QPC starts from the initial value I_0, and then decreases, oscillates and finally converges to a value other than I_0. In addition, oscillations in both the occupation probability and the QPC current are observed. This results from the fact that the spin-up electron can tunnel back and forth between the dots. In contrast, if the electron injected into the left dot is spin-down, it cannot hop into the right dot because $\varepsilon_\downarrow \gg \Omega_0$. The electron occupation probability in the right dot is hence zero (see figure 2(b)). The down spin is also reflected in figure 2(d), where the QPC current remains unchanged. Accordingly, one can distinguish between the two initial electron spin states from the variation of the QPC current. In short, if the QPC current decreases from its initial value, the initial spin state is spin-up. Alternatively, if the initial spin state is spin-down in the left dot, the QPC current remains unchanged.

We have repeated the calculation by considering an additional ESR magnetic field. Without such a field, we cannot distinguish between the case with no electron in the left dot from that with a spin-down electron as discussed in section 2.1. Both give rise to no QPC current variation. In the presence of an ESR field on the left dot (i.e., $\Delta_x \neq 0$), for the zero-electron case, the QPC current remains unchanged. However, for an initial spin-down electron in the left dot $|\downarrow_\mathrm{L}\rangle$, it can flip to the spin-up state $|\uparrow_\mathrm{L}\rangle$, induced by the ESR oscillating magnetic field. In contrast, the spin-up electron can hop into the right dot (see figure 3(a)). This leads to a variation in the QPC current (see figure 3(b)). Therefore, these two cases can now be distinguished.

3. Readout of single electron spin: two electrons in the DQD

3.1. Theoretical model

We now study the readout of the electron spin states in the left (qubit) dot assuming that an additional electron initially occupies the right (reference) dot (see figure 4), as in a recent experiment [22]. We further assume that the gate voltages of the dots are tuned so that no two electrons can simultaneously stay in the qubit dot. Thus, the two relevant occupation configurations correspond to two electrons in the right dot or one electron in each dot. The total Hamiltonian is

$$H = H_\mathrm{QPC} + H_\mathrm{DQD} + H_\mathrm{int}, \tag{16}$$

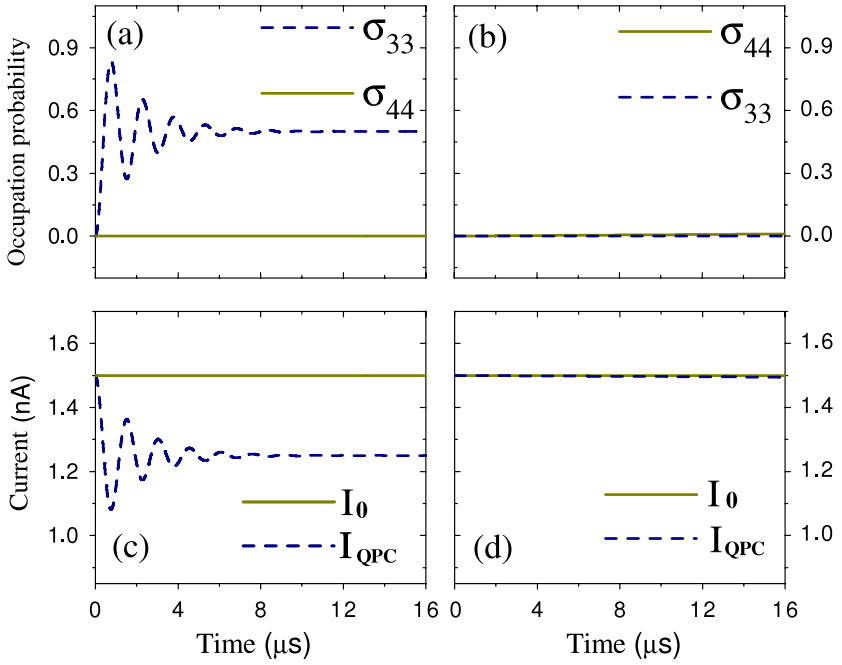

Figure 2. Time evolution of the electron occupation probability in the right dot for (a) spin-up $|\uparrow_{\rm L}\rangle$ and (b) spin-down $|\downarrow_{\rm L}\rangle$ electron states in the left dot. (c) and (d) Time evolution of the QPC currents corresponding to (a) and (b), respectively. We have set the parameters as $\Omega_0 = 0.25\ \mu$eV, $\chi = 0.0025\ \mu$eV and $\Gamma_{\rm d} = 60$ MHz.

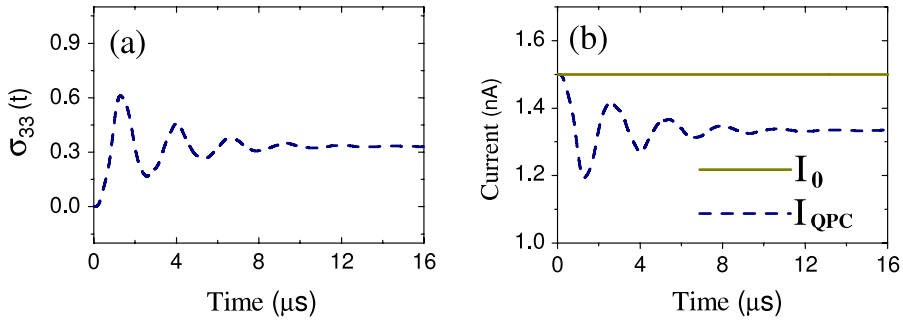

Figure 3. (a) Time evolution of the occupation probability in the spin-up state $|\uparrow_{\rm R}\rangle$ in the right dot in the presence of an oscillating magnetic field. Initially, the electron in the left dot is in the spin-down state $|\downarrow_{\rm L}\rangle$. (b) The corresponding time evolution of the QPC current. We have taken $\Delta_x = 0.3\ \mu$eV, and $\omega = 0.5\ \mu$eV.

where $H_{\rm QPC}$ is the Hamiltonian of the QPC in the two-electron case, which has the same form as equation (3), but with Ω_{lr} replaced by Ω'_{lr}. The Hamiltonian of the isolated DQD system after considering both inter- and intra-dot Coulomb interactions now becomes

$$H_{\rm DQD} = H_0 + H_{\rm spin}, \tag{17}$$

where

$$H_0 = \sum_{i\sigma} E_i c^+_{i\sigma} c_{i\sigma} + \Omega_0 \sum_{\sigma} (c^+_{\rm L\sigma} c_{\rm R\sigma} + {\rm H.c.}) + \sum_i U_i n_{i\uparrow} n_{i\downarrow} + U_{\rm LR} \sum_{\sigma\sigma'} n_{\rm L\sigma} n_{\rm R\sigma'}. \tag{18}$$

In the absence of a net nuclear polarization, randomly oriented and fluctuating nuclear spins in the host materials give rise to effective magnetic fields $\mathbf{B_{NL}}$ and $\mathbf{B_{NR}}$ in the left and right dot, respectively. They results from different local environments for the electrons in the respective dots. However, nuclear fields change with a nuclear spin relaxation timescale of the order 1 s, which is much longer than any timescales characterizing the transport processes of electron. These nuclear effective fields can thus be regarded as static fields in our discussion [23–25]. Therefore, we can describe the influence of the magnetic fields on the electron spins in the DQD by

$$H_{\rm spin} = g\mu_{\rm B}\mathbf{B}_{\rm NL}\cdot\mathbf{S}_{\rm L} + g\mu_{\rm B}\mathbf{B}_{\rm NR}\cdot\mathbf{S}_{\rm R} + g\mu_{\rm B}B^{\rm z}_{\rm ext}(S^{\rm z}_{\rm L} + S^{\rm z}_{\rm R}) + g\mu_{\rm B}B^{\rm x}_{\rm L}\cos(\omega_{\rm c}t)S^{\rm x}_{\rm L}, \tag{19}$$

where $\mathbf{S}_{\rm L}$ and $\mathbf{S}_{\rm R}$ correspond to the electron spin in the left and right dots, respectively. The third term in equation (19) is the Zeeman splitting caused by an external perpendicular field. The last term is an ESR oscillating magnetic field in the x direction. In the present discussion, we assume that the ESR oscillating magnetic field is only applied on the qubit dot.

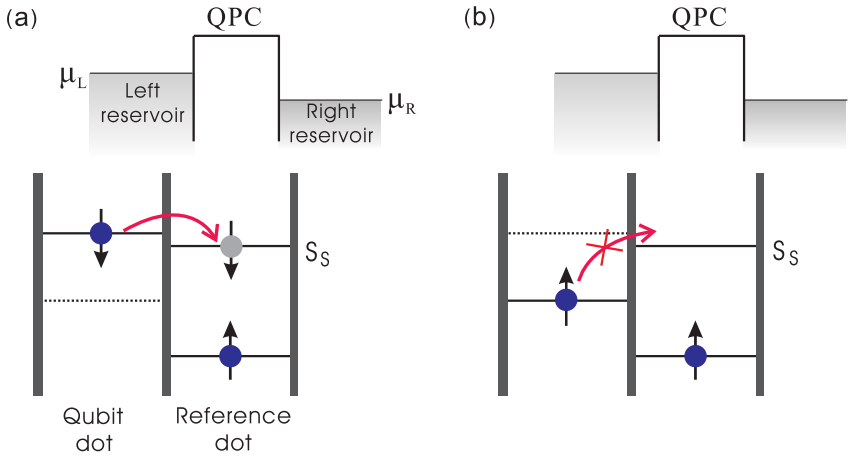

Figure 4. Schematic diagram of a double quantum dot (DQD) and a quantum point contact (QPC) with two electrons in the DQD. One spin-up electron is initially kept in the reference dot by properly adjusting the gate voltages. (a) A spin-down electron in the left dot can always hop into the right dot after taking hyperfine interactions into account. (b) Transport of a spin-up electron is forbidden due to Pauli exclusion.

The relevant electronic states for the DQD span a five-dimensional Hilbert space. The basis set consists of double-dot triplets $|1\rangle \equiv |T_+\rangle = |\uparrow_{\rm L}\uparrow_{\rm R}\rangle$, $|2\rangle \equiv |T_-\rangle = |\downarrow_{\rm L}\downarrow_{\rm R}\rangle$, and $|3\rangle \equiv |T_0\rangle = \frac{1}{\sqrt{2}}(|\uparrow_{\rm L}\downarrow_{\rm R}\rangle + |\downarrow_{\rm L}\uparrow_{\rm R}\rangle)$, double-dot singlet $|4\rangle \equiv |S_{\rm D}\rangle = \frac{1}{\sqrt{2}}(|\uparrow_{\rm L}\downarrow_{\rm R}\rangle - |\downarrow_{\rm L}\uparrow_{\rm R}\rangle)$, and single-dot singlet $|5\rangle \equiv |S_{\rm S}\rangle = \frac{1}{\sqrt{2}}(|\uparrow_{\rm R}\downarrow_{\rm R}\rangle - |\downarrow_{\rm R}\uparrow_{\rm R}\rangle)$. Single-dot triplet states are excluded due to their much higher orbital energies [26, 11]. In this representation, $H_{\rm DQD}$ is rewritten as

$$\begin{aligned} H_{\rm DQD} = & \sum_{i=1,2,3,4,5} E_i|i\rangle\langle i| \\ & + \frac{g\mu_{\rm B}}{\sqrt{2}}\big[(B_{\rm s}^x + {\rm i}B_{\rm s}^y)|3\rangle\langle 1| + (B_{\rm s}^x - {\rm i}B_{\rm s}^y)|3\rangle\langle 2| + {\rm H.c.}\big] \\ & + \frac{g\mu_{\rm B}}{\sqrt{2}}\big[(-B_{\rm d}^x - {\rm i}B_{\rm d}^y)|4\rangle\langle 1| + (B_{\rm d}^x - {\rm i}B_{\rm d}^y)|4\rangle\langle 2| + {\rm H.c.}\big] \\ & + \Omega_0(|4\rangle\langle 5| + |5\rangle\langle 4|) + g\mu_{\rm B}B_{\rm d}^z\big(|3\rangle\langle 4| + |4\rangle\langle 3|\big) \\ & + \Omega_1\cos(\omega_c t)\big[|3\rangle\langle 1| + |3\rangle\langle 2| - |4\rangle\langle 1| + |4\rangle\langle 2| \\ & + {\rm H.c.}\big], \end{aligned} \tag{20}$$

where $\mathbf{B}_{\rm d} = \frac{1}{2}(\mathbf{B}_{\rm NL} - \mathbf{B}_{\rm NR})$, $\mathbf{B}_{\rm s} = \frac{1}{2}(\mathbf{B}_{\rm NL} + \mathbf{B}_{\rm NR}) + B_{\rm ext}^z\tilde{\mathbf{z}}$, and $\Omega_1 = \frac{1}{2\sqrt{2}}g\mu_{\rm B}B_{\rm L}^x$. We have also introduced energy levels given by

$$E_{1,2} = E_3 \mp g\mu_{\rm B}B_{\rm s}^z, \qquad E_{3,4} = E_{\rm L} + E_{\rm R} + U_{\rm LR}, \tag{21}$$

and

$$E_5 = 2E_{\rm R} + U_{\rm R}. \tag{22}$$

A critical step in the readout is the hopping to the right dot, where there is a nonzero Coulomb energy barrier

$$\Delta = E_5 - E_4 = U_{\rm R} - U_{\rm LR} - (E_{\rm L} - E_{\rm R}), \tag{23}$$

for the second electron at the right dot if the intra-dot repulsion $U_{\rm R}$ dominates.

The interaction Hamiltonian between the DQD and the QPC is

$$H_{\rm int} = \sum_{lrk\sigma}\delta\Omega'_{lr}c^\dagger_{{\rm R}\sigma}c_{{\rm R}\sigma}c^\dagger_{{\rm R}\bar\sigma}c_{{\rm R}\bar\sigma}(a^\dagger_{lk}a_{lk} + a^\dagger_{rk}a_{rk}). \tag{24}$$

In the singlet–triplet representation, it can be written as

$$H_{\rm int} = \sum_{lrk}\delta\Omega'|5\rangle\langle 5|(a^\dagger_{lk}a_{rk} + a^\dagger_{rk}a_{lk}). \tag{25}$$

Similar to the one-electron case, the hopping amplitude Ω'_{lr} of the QPC and its change $\delta\Omega'_{lr}$ by either adding or removing an electron in the right dot are assumed to be energy-independent, so that $\Omega'_{lr}(E_l, E_r) \equiv \Omega'$ and $\Omega'_{lr} + \delta\Omega'_{lr} \equiv \Omega''$. As discussed in the one-electron case, the left QD is a qubit dot and the right dot is a reference dot. The nearby QPC works as a detector to measure the number change of electrons in the reference dot. When one electron stays in the reference dot, the current flowing through the detector is I_1. For double occupancy in the reference dot, the detector current becomes I_2, where $I_2 < I_1$ because of the increased QPC barrier induced by the additional electron. As a result, the variation of the electron number in the reference dot can be reliably detected from the current change of the detector.

We first briefly discuss the readout processes of the qubit states. We assume that the electron that is always kept in the right dot is spin-up. This can be realized by injecting an unpolarized electron and wait for a time interval much longer than the typical relaxation time of a single electron spin. It will relax to its ground spin-up state due to its coupling to the outside environment. An additional electron is then injected into the qubit dot and its spin state will be readout. For a spin-down qubit electron, the initial total spin in the z direction is $S_z = 0$. The DQD system takes either the double electron state $|3\rangle$ or $|4\rangle$ with an equal probability of $1/2$. If the state taken is $|4\rangle$, the electron can directly hop onto the right dot. This hopping is described by the Ω_0 term in equation (20). Otherwise, if it is $|3\rangle$, the electron can transit to state $|4\rangle$, as allowed by the $B_{\rm d}^z$ term in equation (20). Then hopping into the right dot becomes similarly possible. Therefore, the qubit electron can always hop onto the reference dot on the right, leading to the state $|5\rangle$ for $S_z = 0$. Due to this hopping, the QPC current changes from I_1 to another value and this indicates the spin-down qubit state.

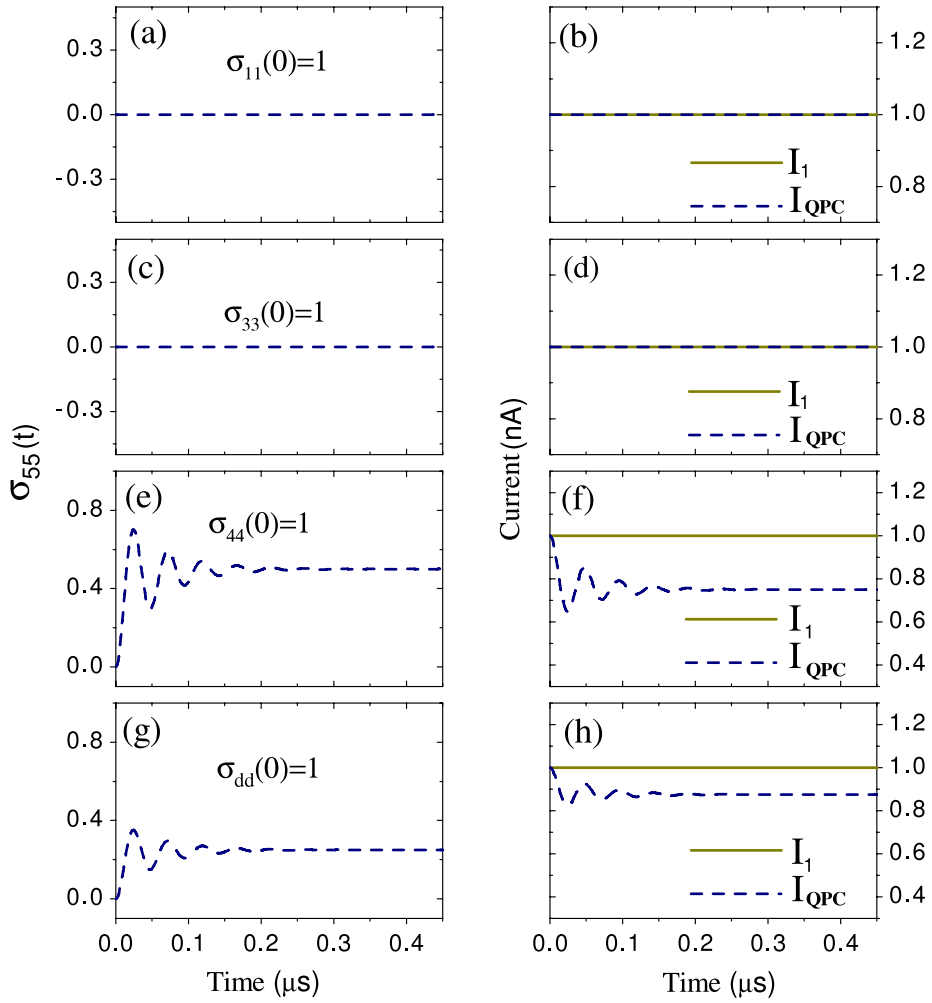

Figure 5. Time evolution of the occupation probability $\sigma_{55}(t)$ for the single-dot singlet state $|S_S\rangle$ with four different initial conditions: (a) $\sigma_{11}(0) = 1$, (c) $\sigma_{33}(0) = 1$, (e) $\sigma_{44}(0) = 1$ and (g) $\sigma_{dd}(0) = 1$, where the hyperfine interaction is not considered. (b), (d), (f) and (h) The corresponding QPC currents. Here we have chosen the following parameters: $B_{\rm NL}^{x,y,z} = (0, 0, 0)$ mT, $B_{\rm NR}^{x,y,z} = (0, 0, 0)$ mT, $\omega_c = 3.75$ μeV, $\Delta = 0.25$ μeV, $\Omega_0 = 0.25$ μeV, $\chi' = 0.0025$ μeV, $\Omega_1 = 0.375$ μeV, and $\Gamma_d' = 60$ MHz.

In contrast, for a spin-up qubit electron leading to a total spin component $S_z = 1$, it forms the triplet state $|1\rangle$ with the spin-up electron in the reference dot. Because of the application of a large external magnetic field $B_{\rm ext}^z \gg \sqrt{\langle B_N^2\rangle}$, this triplet state $|1\rangle$ is far away in energy from other states. Thus, it is decoupled from states $|3\rangle$ or $|4\rangle$ and the electron in the left dot cannot hop to the right dot. Therefore, the current flowing through the QPC remains constant at I_1 and this indicates that the initial qubit state is spin-up.

3.2. Bloch-type rate equation

To reveal the quantum dynamics of electron states in the DQD system, we derive a set of Bloch-type rate equations for the reduced density matrix $\sigma(t)$ of the DQD, also using the technique developed by Gurvitz *et al* [18]. We assume the high Zeeman splitting limit, i.e., $B_{\rm ext}^z \gg \sqrt{\langle B_N^2\rangle}$, in order to suppress the effect of the nuclear fields. Spin flips caused by hyperfine interactions are then negligible. The many-body wavefunction $|\Psi(t)\rangle$ of the whole system in the singlet–triplet basis is given by

$$|\Psi(t)\rangle = \sum_{i=1,2,3,4,5} \Big[b_i(t)c_i^+ + \sum_{lr} b_{ilr}(t)c_{ilr}^+ a_r^\dagger a_l + \sum_{l<l',r<r'} b_{ill'rr'}(t)c_i^+ a_r^\dagger a_{r'} a_l a_{l'} + \cdots \Big]|0\rangle, \tag{26}$$

where $|0\rangle$ is the vacuum state and $b_j(t)$ are the time-dependent probability amplitudes of the corresponding state $|j\rangle$. For example, when $j = ilr$, with $i = 1, 2, \ldots$ or 5, $b_j(t)$ is the probability amplitude of the state with the DQD system at state $|i\rangle$ after one electron has already passed through the QPC at time t. In addition, we have used $c_i^\dagger$ (c_i), which denotes the creation (annihilation) operator for state $|i\rangle$ in the DQD system.

Substituting the wavefunction $|\Psi(t)\rangle$ (equation (26)) into the Schrödinger equation $i|\dot{\Psi}(t)\rangle = H|\Psi(t)\rangle$, and tracing over the reservoir states of the QPC, we obtain a set of Bloch-type

rate equations for the reduced density matrix $\sigma(t)$ of the DQD system:

$$\begin{aligned}
\dot{\sigma}_{11}(t) &= \mathrm{i}D_-\sigma_{41} - \mathrm{i}S_-\sigma_{31} - \mathrm{i}D_+\sigma_{14} + \mathrm{i}S_+\sigma_{13},\\
\dot{\sigma}_{22}(t) &= -\mathrm{i}D_+\sigma_{42} - \mathrm{i}S_+\sigma_{32} + \mathrm{i}D_-\sigma_{24} + \mathrm{i}S_-\sigma_{23},\\
\dot{\sigma}_{33}(t) &= \mathrm{i}\Omega_{\mathrm{d}}^z(\sigma_{34} - \sigma_{43}) + \mathrm{i}S_+\sigma_{32} + \mathrm{i}S_-\sigma_{31}\\
&\quad - \mathrm{i}S_-\sigma_{23} - \mathrm{i}S_+\sigma_{13},\\
\dot{\sigma}_{44}(t) &= \mathrm{i}\Omega_{\mathrm{d}}^z(\sigma_{43} - \sigma_{34}) + \mathrm{i}D_+\sigma_{42} - \mathrm{i}D_-\sigma_{41}\\
&\quad + \mathrm{i}\Omega_0(\sigma_{45} - \sigma_{54}) - \mathrm{i}D_-\sigma_{24} + \mathrm{i}D_+\sigma_{14},\\
\dot{\sigma}_{55}(t) &= \mathrm{i}\Omega_0(\sigma_{54} - \sigma_{45}),
\end{aligned} \tag{27}$$

and

$$\begin{aligned}
\dot{\sigma}_{12}(t) &= \mathrm{i}(E_2 - E_1)\sigma_{12} + \mathrm{i}D_-\sigma_{14} + \mathrm{i}S_-\sigma_{13}\\
&\quad + \mathrm{i}D_-\sigma_{42} - \mathrm{i}S_-\sigma_{32},\\
\dot{\sigma}_{13}(t) &= \mathrm{i}(E_3 - E_1)\sigma_{13} + \mathrm{i}D_-\sigma_{43} - \mathrm{i}S_-\sigma_{33} + \mathrm{i}S_+\sigma_{12}\\
&\quad + \mathrm{i}S_-\sigma_{11} + \mathrm{i}\Omega_{\mathrm{d}}^z\sigma_{14},\\
\dot{\sigma}_{14}(t) &= \mathrm{i}(E_4 - E_1)\sigma_{14} + \mathrm{i}D_-(\sigma_{44} - \sigma_{11}) - \mathrm{i}S_-\sigma_{34}\\
&\quad + \mathrm{i}D_+\sigma_{12} + \mathrm{i}\Omega_0\sigma_{15} + \mathrm{i}\Omega_{\mathrm{d}}^z\sigma_{13},\\
\dot{\sigma}_{15}(t) &= \mathrm{i}(E_5 - E_1)\sigma_{15} + \mathrm{i}\Omega_0\sigma_{14} + \mathrm{i}D_-\sigma_{45} - \mathrm{i}S_-\sigma_{35}\\
&\quad - \tfrac{1}{2}\Gamma_{\mathrm{d}}'\sigma_{15} - \tfrac{1}{2}\chi'\sigma_{14}.\\
\dot{\sigma}_{23}(t) &= \mathrm{i}(E_3 - E_2)\sigma_{23} - \mathrm{i}D_+\sigma_{43} - \mathrm{i}S_+(\sigma_{33} - \sigma_{22})\\
&\quad + \mathrm{i}S_-\sigma_{21} + \mathrm{i}\Omega_{\mathrm{d}}^z\sigma_{24},\\
\dot{\sigma}_{24}(t) &= \mathrm{i}(E_4 - E_2)\sigma_{24} - \mathrm{i}D_+(\sigma_{44} - \sigma_{22}) - \mathrm{i}S_+\sigma_{34}\\
&\quad - \mathrm{i}D_-\sigma_{21} + \mathrm{i}\Omega_0\sigma_{25} + \mathrm{i}\Omega_{\mathrm{d}}^z\sigma_{23},\\
\dot{\sigma}_{25}(t) &= \mathrm{i}(E_5 - E_2)\sigma_{25} + \mathrm{i}\Omega_0\sigma_{24} - \mathrm{i}D_+\sigma_{45} - \mathrm{i}S_+\sigma_{35}\\
&\quad - \tfrac{1}{2}\Gamma_{\mathrm{d}}'\sigma_{25} - \tfrac{1}{2}\chi'\sigma_{24},\\
\dot{\sigma}_{34}(t) &= -\mathrm{i}S_-\sigma_{24} - \mathrm{i}S_+\sigma_{14} - \mathrm{i}D_-\sigma_{31} + \mathrm{i}D_+\sigma_{32}\\
&\quad - \mathrm{i}\Omega_{\mathrm{d}}^z(\sigma_{44} - \sigma_{33}) + \mathrm{i}\Omega_0\sigma_{35},\\
\dot{\sigma}_{35}(t) &= \mathrm{i}(E_5 - E_3)\sigma_{35} + \mathrm{i}\Omega_0\sigma_{34} - \mathrm{i}S_-\sigma_{25} - \mathrm{i}S_+\sigma_{15}\\
&\quad - \mathrm{i}\Omega_{\mathrm{d}}^z\sigma_{45} - \tfrac{1}{2}\Gamma_{\mathrm{d}}'\sigma_{35} - \tfrac{1}{2}\chi'\sigma_{34},\\
\dot{\sigma}_{45}(t) &= \mathrm{i}(E_5 - E_4)\sigma_{45} + \mathrm{i}\Omega_0(\sigma_{44} - \sigma_{55}) - \mathrm{i}D_-\sigma_{25}\\
&\quad + \mathrm{i}D_+\sigma_{15} - \mathrm{i}\Omega_{\mathrm{d}}^z\sigma_{35} - \tfrac{1}{2}\Gamma_{\mathrm{d}}'\sigma_{45} - \tfrac{1}{2}\chi'(\sigma_{44} + \sigma_{55}).
\end{aligned} \tag{28}$$

Here the detector-induced dephasing rate is $\Gamma_{\mathrm{d}}' = (\sqrt{D''} - \sqrt{D'})^2$, with

$$D'' = 2\pi\rho_{\mathrm{L}}\rho_{\mathrm{R}}\Omega''^2 V_{\mathrm{d}}, \qquad D' = 2\pi\rho_{\mathrm{L}}\rho_{\mathrm{R}}\Omega'^2 V_{\mathrm{d}}. \tag{29}$$

Also, we have defined

$$\begin{aligned}
\chi' &= \frac{\Lambda'}{V_{\mathrm{d}}}\left(\frac{\Omega'}{\Omega''} + \frac{\Omega''}{\Omega'} - 2\right), \qquad \Omega_{\mathrm{d}}^z = g\mu_{\mathrm{B}}B_{\mathrm{d}}^z,\\
D_\pm(t) &= \Omega_{\mathrm{d}}^\pm + \Omega_1(t), \qquad S_\pm(t) = \Omega_s^\pm + \Omega_1(t),
\end{aligned} \tag{30}$$

where

$$\begin{aligned}
\Lambda' &= 2\pi\rho_{\mathrm{L}}\rho_{\mathrm{R}}\Omega''\Omega_0\Omega' V_{\mathrm{d}},\\
\Omega_1(t) &= \Omega_1\cos(\omega_{\mathrm{c}}t),\\
\Omega_{\mathrm{d}}^\pm &= \frac{g\mu_{\mathrm{B}}}{\sqrt{2}}(B_{\mathrm{d}}^x \pm \mathrm{i}B_{\mathrm{d}}^y),\\
\Omega_s^\pm &= \frac{g\mu_{\mathrm{B}}}{\sqrt{2}}(B_{\mathrm{s}}^x \pm \mathrm{i}B_s^y).
\end{aligned} \tag{31}$$

The QPC current is given by

$$I(t) = I_1[\sigma_{11}(t) + \sigma_{22}(t) + \sigma_{33}(t) + \sigma_{44}(t)] + I_2\sigma_{55}(t), \tag{32}$$

where I_1 (I_2) is the stationary current through the QPC when the right dot is occupied by one electron (two electrons).

3.3. Results and analysis

We have numerically integrated the rate equations and obtained the time-dependent density matrix elements. As discussed in section 3.1, since there is always a spin-up electron in the reference dot, the injection of a spin-up electron into the qubit dot forms a double-dot triplet state $|1\rangle = |\uparrow_{\mathrm{L}}\uparrow_{\mathrm{R}}\rangle$ in the DQD system. In contrast, if the injected electron is spin-down, the DQD system initially takes the state $|\downarrow_{\mathrm{L}}\uparrow_{\mathrm{R}}\rangle$. Thus, after injecting an electron into the left dot, the possible experimental initial states of the DQD system are $|1\rangle$ and $|\downarrow_{\mathrm{L}}\uparrow_{\mathrm{R}}\rangle$. In order to show how the current through the QPC changes for different initial states of the DQD system, we assume that the DQD system initially takes the state $|1\rangle$ or $|\downarrow_{\mathrm{L}}\uparrow_{\mathrm{R}}\rangle$.

The initial state $|\downarrow_{\mathrm{L}}\uparrow_{\mathrm{R}}\rangle$ is a superposition of the double-dot triplet state $|3\rangle$ and the double-dot singlet state $|4\rangle$, i.e.,

$$|\downarrow_{\mathrm{L}}\uparrow_{\mathrm{R}}\rangle = \frac{1}{\sqrt{2}}(|3\rangle - |4\rangle). \tag{33}$$

Here the state $|4\rangle$ is coupled to the single-dot singlet state $|5\rangle$ directly via hopping coupling, while the state $|3\rangle$ is coupled to $|5\rangle$ via the intermediate state $|4\rangle$ (where the transition from $|3\rangle$ to $|4\rangle$ is induced by the B_{d}^z term). To reveal the contributions from different components, we also take the state $|3\rangle$ or $|4\rangle$ as the initial state to study the time evolution of the current through the QPC.

In our numerical calculations regarding the initial state $|\downarrow_{\mathrm{L}}\uparrow_{\mathrm{R}}\rangle$, we rewrite the rate equations (27) and (28) in the occupation representation defined by the basis states $|a\rangle$, $|b\rangle$, $|c\rangle$, $|d\rangle$, and $|e\rangle$, where

$$\begin{aligned}
|a\rangle &\equiv |\uparrow_{\mathrm{L}}\uparrow_{\mathrm{R}}\rangle = |1\rangle,\\
|b\rangle &\equiv |\downarrow_{\mathrm{L}}\downarrow_{\mathrm{R}}\rangle = |2\rangle,\\
|c\rangle &\equiv |\uparrow_{\mathrm{L}}\downarrow_{\mathrm{R}}\rangle = \frac{1}{\sqrt{2}}(|3\rangle + |4\rangle),\\
|d\rangle &\equiv |\downarrow_{\mathrm{L}}\uparrow_{\mathrm{R}}\rangle = \frac{1}{\sqrt{2}}(|3\rangle - |4\rangle),\\
|e\rangle &\equiv \frac{1}{\sqrt{2}}(|\uparrow_{\mathrm{R}}\downarrow_{\mathrm{R}}\rangle - |\downarrow_{\mathrm{R}}\uparrow_{\mathrm{R}}\rangle) = |5\rangle.
\end{aligned} \tag{34}$$

With these new basis states, one can express $\sigma_{ij} \equiv \langle i|\sigma|j\rangle$ ($i, j = 1$ to 5) using $\sigma_{\mu\nu} \equiv \langle\mu|\sigma|\nu\rangle$ ($\mu, \nu = a, b, c, d$, and e), e.g.,

$$\begin{aligned}
\sigma_{13} &= \frac{1}{\sqrt{2}}(\sigma_{ac} + \sigma_{ad}),\\
\sigma_{23} &= \frac{1}{\sqrt{2}}(\sigma_{bc} + \sigma_{bd}),\\
\sigma_{33} &= \tfrac{1}{2}(\sigma_{cc} + \sigma_{cd} + \sigma_{dc} + \sigma_{dd}),\\
\sigma_{43} &= \tfrac{1}{2}(\sigma_{cc} + \sigma_{cd} - \sigma_{dc} - \sigma_{dd}).
\end{aligned} \tag{35}$$

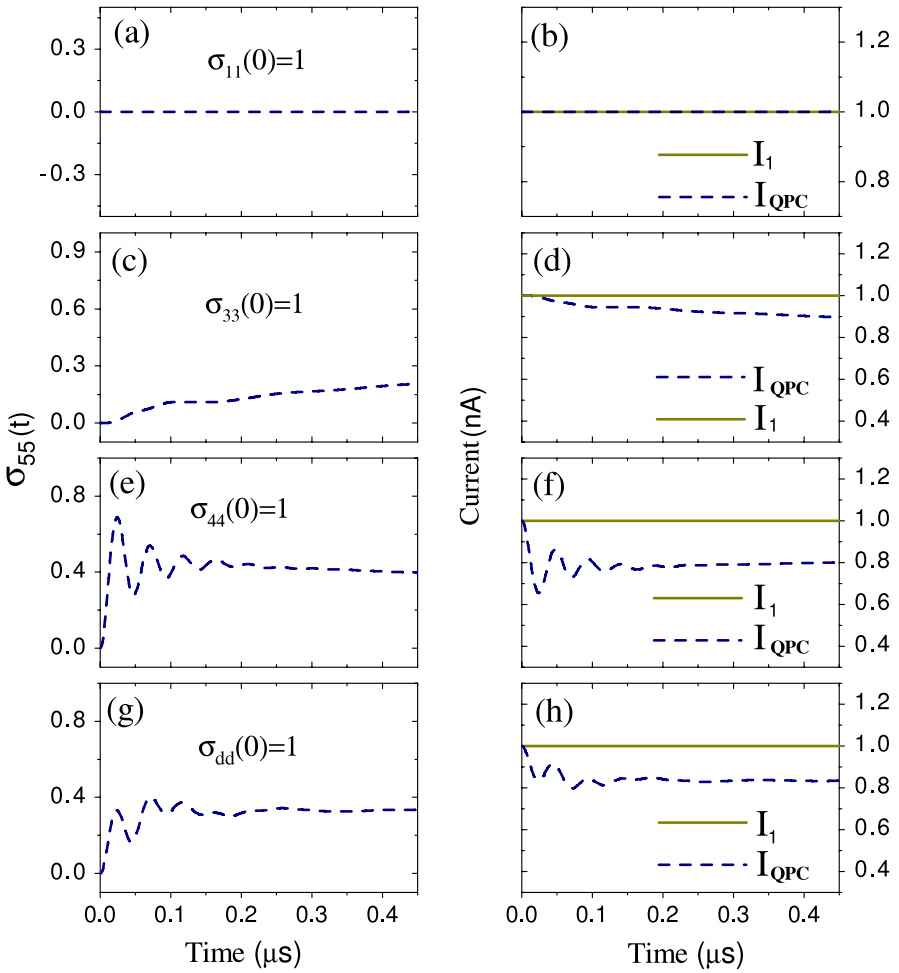

Figure 6. Time evolution of the occupation probability $\sigma_{55}(t)$ of the single-dot singlet state $|S_S\rangle$ for four different initial conditions: (a) $\sigma_{11}(0) = 1$, (c) $\sigma_{33}(0) = 1$, (e) $\sigma_{44}(0) = 1$ and (g) $\sigma_{dd}(0) = 1$, where the hyperfine interaction is included. (b), (d), (f) and (h) The corresponding QPC currents for these four different initial conditions. The nuclear magnetic fields are chosen to be $B_{\rm NL}^{x,y,z} = (-2, 1, 3)$ mT, and $B_{\rm NR}^{x,y,z} = (-1, 2, 0)$ mT. The other parameters are the same as in figure 5.

In this way, we can transform equations (27) and (28) into the rate equations in the occupation representation.

We first consider the case without hyperfine interactions, i.e., $\mathbf{B}_{\rm NL(R)} = 0$. In this limit, the coupling between the states $|3\rangle$ and $|4\rangle$ vanishes. (i) If initially the DQD takes the double-dot triplet state $|1\rangle$, the system will not evolve into other states due to the large Zeeman splitting. In this case, the electron in the left dot does not hop into the right one and the current through the QPC does not change, as shown in figures 5(a) and (b). (ii) Alternatively, for an initial state $|3\rangle$, the DQD system will also remain at this state because $|3\rangle$ does not couple with any other states. Similar to the case of the initial state $|1\rangle$, the occupation probability of the single-dot singlet state $|5\rangle$ is zero and the current through the QPC also remains unchanged (see figures 5(c) and (d)). (iii) In contrast, as shown in figures 5(e) and (f), if the DQD system initially stays at $|4\rangle$, it couples with the single-dot singlet state due to the hopping coupling between the two dots. This gives rise to nonzero occupation probability for the single-dot singlet state and a variable current through the QPC. (iv) The results shown in figures 5(g) and (h) look like a combination of the results in both (ii) and (iii). This is because the initial state $|d\rangle = |\downarrow_{\rm L}\uparrow_{\rm R}\rangle$ is a superposition of the states $|3\rangle$ and $|4\rangle$ (cf equation (33)). Moreover, only the state $|4\rangle$ contributes to the variations of both the probability of the state $|5\rangle$ and the current through the QPC.

Moreover, it is shown in figures 5(b) and (d) that the two cases with initial states $|1\rangle$ and $|3\rangle$ are indistinguishable in measuring the electron spin. This is due to neglecting the hyperfine interactions. When they are included, these two cases become distinguishable (cf figure 6).

For an initial state $|1\rangle$ or $|4\rangle$, the results are similar to those without the hyperfine interactions. This can be clearly seen by comparing figures 6(a) and (b) with figures 5(a) and (b) for initial state $|1\rangle$, and similarly comparing figures 6(e) and (f) with figures 5(e) and (f) for initial state $|4\rangle$. In contrast, for initial state $|3\rangle$, because $|3\rangle$ and $|4\rangle$ are degenerate, hyperfine interactions are able to provide significant couplings. Moreover, state $|4\rangle$ is also coupled to $|5\rangle$ via hopping. Thus, from initial state $|3\rangle$, the system can finally evolve to $|5\rangle$. Indeed, this is reflected in the variations of both the occupation probability of state $|5\rangle$ and the QPC current (comparing figures 6(c) and (d) with figures 5(c) and (d)). For the initial state $|d\rangle = |\downarrow_{\rm L}\uparrow_{\rm R}\rangle$, the probability of the state $|5\rangle$ and the

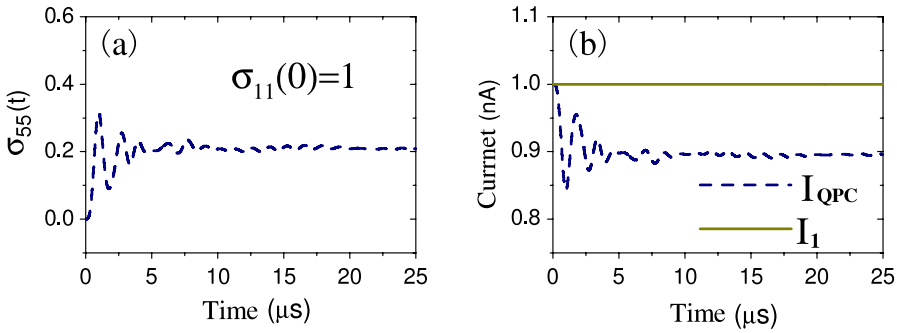

Figure 7. (a) Time evolution of the occupation probability of the single-dot singlet state in the presence of an ESR magnetic field for the initial state $|1\rangle$ (see the text). (b) The corresponding QPC current.

QPC current (shown in figures 6(g) and (h)) also look like a combination of the results for both the initial states $|3\rangle$ and $|4\rangle$ (shown in figures 6(c)–(f)), similar to the case without hyperfine interaction in the DQD.

The last issue to be addressed is to determine if the electron is successfully injected into the left dot. If the injection fails, the QPC current is always I_1. The result is the same as that with a spin-up electron injected into the qubit dot. To distinguish between these two cases, we can apply a transverse magnetic field to flip the electron spin in the qubit dot. For a successful injection, the electron with spin-up will flip to become spin-down and then hop into the right dot. The DQD system then takes the state $|\downarrow_L\uparrow_R\rangle$. As discussed above, this state, i.e., the superposition state of $|3\rangle$ and $|4\rangle$, is coupled to the single-dot singlet state $|5\rangle$, giving rise to a variation of the occupation probability σ_{55} (see figure 7(a)) as well as the QPC current (see figure 7(b)). This is different from the case of a constant current in the absence of any successful electron injection into the left dot.

4. Conclusion

In summary, we have studied the readout of a single electron spin in a DQD system. The electron spin is initially confined in the QD serving as a qubit dot. A reference dot is coupled to the qubit dot via a tunneling coupling. Also, a QPC acts as a measurement device, placed near the reference dot for detecting the variation of the electron number in the reference dot. We have considered the two implementations in which either one or two electrons occupy the DQD. In the one-electron case, the only electron in the DQD is the qubit electron to be measured. An external magnetic field is applied to both dots so that the energy-level splittings $\varepsilon_\uparrow$ and $\varepsilon_\downarrow$ for spin-up and spin-down electrons are different. Gate voltages of the two dots are tuned so that $\varepsilon_\uparrow \sim 0$ and $\varepsilon_\downarrow \gg \Omega_0$. These conditions ensure that only a spin-up electron but not a spin-down electron in the qubit dot can tunnel to the reference dot. This gives rise to very different currents through the QPC and can be used to readout the electron spin states of the qubit dot. In the two-electron case, an additional spin-up electron is always confined in the reference dot. This can be easily achieved by properly tuning the gate voltages of the dots. We have shown that the electron spin states of the qubit dot can also be read out by applying an external magnetic field when considering effects of hyperfine interactions between the electron spin and the nuclear spins of the host materials. In the high Zeeman splitting limit, the flipping of the electron spin induced by the hyperfine interactions are greatly suppressed. In this case, only a spin-down electron in the qubit dot can tunnel to the reference dot. This again allows one to distinguish between the electron spin states in the qubit dot by measuring the currents through the QPC. Furthermore, we propose an approach involving an ESR oscillating magnetic field which can confirm the success of an electron injection event into the qubit dot.

Acknowledgments

This work was supported by the SRFDP, the PCSIRT, NFRPC grant No. 2006CB921205 and the National Natural Science Foundation of China grant Nos 10534060 and 10625416.

References

[1] Hanson R, Witkamp B, Vandersypen L M K, Willems van Beveren L H, Elzerman J M and Kouwenhoven L P 2003 *Phys. Rev. Lett.* **91** 196802
[2] Loss D and DiVincenzo D P 1998 *Phys. Rev.* A **57** 120
[3] Yao W, Liu R-B and Sham L J 2006 *Phys. Rev.* B **74** 195301
[4] Yao W, Liu R-B and Sham L J 2007 *Phys. Rev. Lett.* **98** 077602
[5] Liu R-B, Yao W and Sham L J 2007 *New J. Phys.* **9** 226
[6] Bracker A S, Stinaff E A, Gammon D, Ware M E, Tischler J G, Shabaev A, Efros AI L, Park D, Gershoni D, Korenev V L and Merkulov A 2005 *Phys. Rev. Lett.* **94** 047402
[7] Koppens F H L, Folk J A, Elzerman J M, Hanson R, Willems van Beveren L H, Vink I T, Tranitz H P, Wegscheider W, Kouwenhoven L P and Vandersypen L M K 2005 *Science* **309** 1346
[8] Cheng J, Wu Y, Xu X, Sun D, Steel D G, Bracker A S, Gammon D, Yao W and Sham L J 2006 *Solid State Commun.* **140** 381
[9] Fujisawa T, Austing D G, Tokura Y, Hirayama Y and Tarucha S 2002 *Nature* **419** 278
[10] Elzerman J M, Hanson R, Willems van Beveren L H, Witkamp B, Vandersypen L M K and Kouwenhoven L P 2004 *Nature* **430** 431
[11] Johnson A C, Petta J R, Taylor J M, Yacoby A, Lukin M D, Marcus C M, Hanson M P and Gossard A C 2005 *Nature* **435** 925
[12] Nielsen M A and Chuang I L 2000 *Quantum Computation and Quantum Information* (New York: Cambridge University Press)

[13] Hanson R, Willems van Beveren L H, Vink I T, Elzerman J M, Naber W J M, Koppens F H L, Kouwenhoven L P and Vandersypen L M K 2005 *Phys. Rev. Lett.* **94** 196802
[14] Engel H-A, Golovach V N, Loss D, Vandersypen L M K, Elzerman J M, Hanson R and Kouwenhoven L P 2004 *Phys. Rev. Lett.* **93** 106804
[15] Barrett S D and Stace T M 2006 *Phys. Rev. Lett.* **96** 017405
[16] Field M, Smith C G, Pepper M, Ritchie D A, Frost J E F, Jones G A C and Hasko D G 1993 *Phys. Rev. Lett.* **70** 1311
[17] Pioro-Ladrière M, Tokura Y, Obata T, Kubo T and Tarucha S 2007 *Appl. Phys. Lett.* **90** 024105
[18] Gurvitz S A and Prager Ya S 1996 *Phys. Rev.* B **53** 15932
[19] Gurvitz S A 1997 *Phys. Rev.* B **56** 15215
[20] Ouyang S-H, Lam C-H and You J Q 2006 *J. Phys.: Condens. Matter* **18** 11551
[21] van der Wiel W G, Franceschi S D, Elzerman J M, Fujisawa T, Tarucha S and Kouwenhoven L P 2003 *Rev. Mod. Phys.* **75** 1
[22] Koppens F H L, Buizert C, Tielrooij K J, Vink I T, Nowack K C, Meunier T, Kouwenhoven L P and Vandersypen L M K 2006 *Nature* **442** 766
[23] Coish W A and Loss D 2004 *Phys. Rev.* B **70** 195340
[24] de Sousa R and Sarma S D 2003 *Phys. Rev.* B **67** 033301
[25] Paget D, Lampel G, Sapoval B and Safarov V I 1977 *Phys. Rev.* B **15** 5780
[26] Ashoori R C, Stormer H L, Weiner J S, Pfeiffer L N, Baldwin K W and West K W 1993 *Phys. Rev. Lett.* **71** 613